2013 IEEE/RSJ International Conference on
Intelligent Robots and Systems (IROS)
November 3-7, 2013. Tokyo, Japan

Free-Space Locomotion with Thread Formation

Liyu Wang, Utku Culha and Fumiya Iida

***Abstract*— The paper presents a new concept of locomotion for wheeled or legged robots through an object-free space. The concept is inspired by the behaviour of spiders forming silk threads to move in 3D space. The approach provides the possibility of variation in thread diameter by deforming source material, therefore it is useful for a wider coverage of payload by mobile robots. As a case study, we propose a technology for descending locomotion through a free space with inverted formation of threads in variable diameters. Inverted thread formation is enabled with source material thermoplastic adhesive (TPA) through thermally-induced phase transition. To demonstrate the feasibility of the technology, we have designed and prototyped a 300-gram wheeled robot that can supply and deform TPA into a thread and descend with the thread from an existing hanging structure. Experiment results suggest repeatable inverted thread formation with a diameter range of 1.1-4.5 mm, and a locomotion speed of 0.73 cm per minute with a power consumption of 2.5 W.**

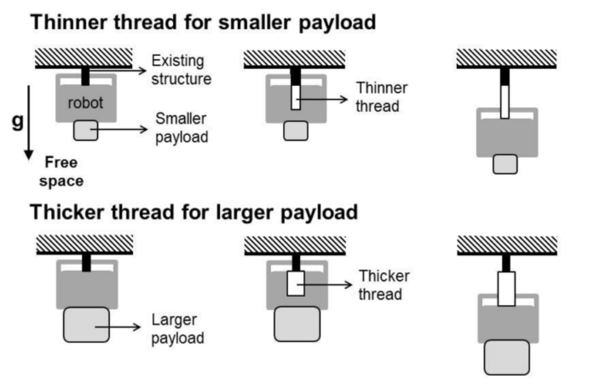

Fig. 1. Concept of free-space robotic locomotion with thread formation. A robot holds onto an existing structure or formed thread, and forms a new thread for locomotion.

I. INTRODUCTION

Being able to move in a 3D space is one of the challenges for mobile robots. Climbing technologies have extended a wheeled or legged robot's mobility from ground surfaces or terrains to stairs or vertical surfaces. Some climbing robots could even move on ceilings [1], but none is able to move into an object-free space without the assistance of an existing cable [2, 3] or additional capability of flying [4].

The paper presents a new concept of locomotion for a wheeled or legged robot to move from a solid structure into an object-free space in a controlled manner. The concept is inspired by spiders' behaviour of forming silk threads to move through a 3D space. Natural spider silk generally has a diameter of several microns, and the diameter can be controlled by a valve located at the end of the duct [5]. It has been found that heavier spiders build thicker silks [6]. When this concept is applied to robotic locomotion, controlled thread formation with variable diameters has benefits for a wider coverage of payload by mobile robots. This makes the proposed approach advantageous over using an existing cable with a fixed diameter.

Fig. 1 shows the concept with a case of robotic descending locomotion from an existing solid structure onto the ground with thread formation. A robot carries a payload and holds onto the structure at first. To descend, it first forms a thread inverted and then move on the formed thread. When the payload increases, the robot can increase the diameter of formed threads. From the conceptualization, we can see that the technical challenge being faced is whether a robot is able to control inverted formation of a thread at the same time of holding onto and descending along a formed thread.

A solution to the above problem requires the robot to carry onboard source material that exhibits moderate tensile strength at ambient temperature. As a case study of descending locomotion in room-temperature environment, we have developed a technology with source material thermoplastic adhesive (TPA) due to its plastic property and moderate tensile strength (over 5 MPa at room temperature). TPA is economic, accessible, and has been used in industries for over half a century and increasingly in robotic applications [7, 8]. To demonstrate the feasibility of the proposed technology, we have designed and prototyped a 300-gram wheeled robot that can descend along threads formed by itself from onboard TPA. Various experiments have been carried out with the robot to assess the variability and repeatability of thread formation as well as locomotion performance.

The remainder of the paper is arranged as follows. Section II introduces the process of inverted thread formation with TPA and a model of thermally-induced phase transition. Section III describes the mechatronic design of the prototyped robot. Section IV presents the experiments and the results. Section V gives conclusions and directions for future work.

II. INVERTED THREAD FORMATION WITH PHASE TRANSITION

In the proposed technology, a robot needs to descend through a free-space by forming a thread. This kind of inverted formation of structures is generally challenging because it has to meet two criteria. First, newly added

*This work was supported by the Swiss National Science Foundation Professorship Grant No. PP00P2123387/1, and the ETH Zurich Research Grant ETH-23-10-3.

L. Wang, U. Culha, and F. Iida are with Bio-Inspired Robotics Lab, Department of Mechanical and Process Engineering, ETH Zurich, 8092 Zurich, Switzerland `liyu.wang, utku.culha, fumiya.iida at mavt.ethz.ch`

978-1-4673-6357-0/13/$31.00 ©2013 IEEE

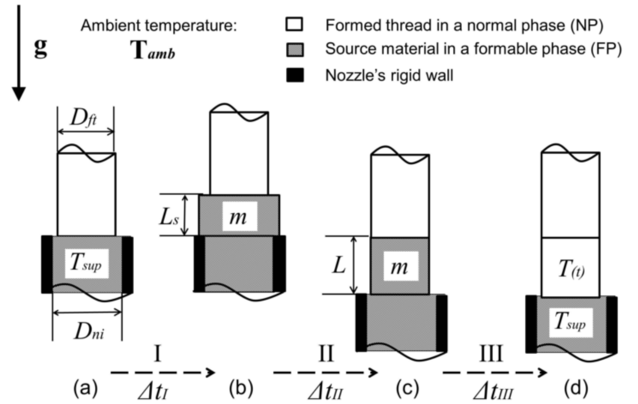

Fig. 2. 2D illustration of one repetition of the overall process of inverted thread formation. (a)-(b) Supply of source material. (b)-(c) Deformation of supplied material into a thread. (c)-(d) Phase transition of the formed thread.

material needs to develop enough adhesion with an existing structure on the top, so that it does not break and fall. Second, a newly formed structure needs to have enough cohesive strength to hold its own shape and weight to avoid collapse.

Our proposed technology adopts a supply-deformation method for inverted thread formation based on extrusion and elongation of source material using a nozzle. The nozzle has two functions. First, it regulates the supply of source material with extrusion, and second it provides a cross-sectional area to develop adhesive stress for elongation of supplied material. The method can be generally described as this: a thread can be formed inverted by repeatedly supplying material from the nozzle to the existing structure above, and then deforming it into a certain diameter under the tensile stress applied by the nozzle. Further detail will be explained in Section II.A.

An important aspect in the proposed technology is the involvement of phase transition of source material. Phase transition of source material can significantly lower the forces needed in supply and deformation, while maintaining the strength of a formed thread to hold the weight of the robot and a potential payload. In the simplest case, we consider the material to have two phases, which we call the normal phase (NP) and the formable phase (FP). In NP, the material has higher values for physical parameters such as modulus, viscosity, strength, and surface energy, etc. Therefore, it is stronger for holding the robot and payload. In FP, the material is weaker with lower values for those parameters, but can still hold its own weight and shape so it is different from fluid. That means a small force can cause material supply and elongation for thread formation. A thermal approach to phase transition will be explained and modelled in Section II.B.

A. Process of Inverted Thread Formation

Fig. 2 illustrates one repetition of the overall process of inverted thread formation. It is assumed that the material starts with FP and there exists a thread segment from the previous repetition. In the first subprocess I, a certain mass m of material is supplied through the nozzle with an inner diameter of D_{ni} upwards onto the lower surface of the already formed thread segment. It pushes the existing thread upwards with a certain distance of L_s with negligible bending. In this subprocess, the material in FP develops adhesion with the existing thread above as well as with the exit of nozzle. It also maintains cohesion with the material still in the nozzle. In the second subprocess II, the supplied material in FP experiences deformation into a certain diameter D_{ft}. Deformation is caused by the tensile stress from adhesion during displacement of nozzle. Assuming deformation of the material is isochoric, the geometrical relationship between the deformed length of the thread L and D_{ft} is:

$$D_{ft} = 2\sqrt{\frac{m}{\pi \rho L}} \tag{1}$$

where ρ is the density of material, and $L > L_s$ results in elongation. In the third subprocess III, the material experiences phase transition from FP to NP. The duration of each subprocess is denoted as Δt_I, Δt_{II}, and Δt_{III}.

TABLE I

PARAMETER VALUES FOR MODELS

Density of TPA ρ	1.0×10^3 kg/m^3
Glass transition temperature of TPA T_g	-20°C
Bond formation temperature of TPA T_{bf}	55°C
Specific heat capacity of TPA c	2500 J/(kg·°C)
Thermal conductivity of TPA K	0.45 W/(m·°C)
Heat transfer coefficient of air h	9 W/(m^2·°C)

B. A Thermal Approach to Phase Transition

In the proposed technology, we adopt a thermal approach to phase transition since aforementioned physical properties of material are all temperature dependent. The temperature dependency of physical parameters is complex, but empirical laws have been developed for thermoplastic materials. For example, for a given thermoplastic polymer, modulus can be approximated as an exponential function of temperature between glass transition temperature T_g and flowing temperature [9]. Viscosity is a WLF function [10] of temperature above T_g since polymers are all amorphous or semi-crystalline. Regarding adhesiveness, it has been reported that adhesive bonding strength of TPA is dependent on the bonding temperature [11]. Above a certain threshold of bonding temperature, sufficient bonding strength can be obtained, and this temperature is usually referred to as bond formation temperature T_{bf} [7].

Based on these relationships, FP corresponds to thermoplastics at a relatively higher temperature T_{sup}, and NP corresponds to the ambient temperature T_{amb}. Phase transition from FP to NP can be realized by cooling, whose dynamics can be explained by Fourier's law for conduction and Newton's cooling law for convection. When temperature gradient is ignored, thermodynamics $T(t)$ of the middle point of the thread under formation during subprocess III may be approximated as:

$$cm\frac{dT(t)}{dt} = -hA_{conv}(T(t){-}T_{amb}){+}\frac{2KA_{cond}}{L}(T_{sup}{-}T(t)) \tag{2}$$

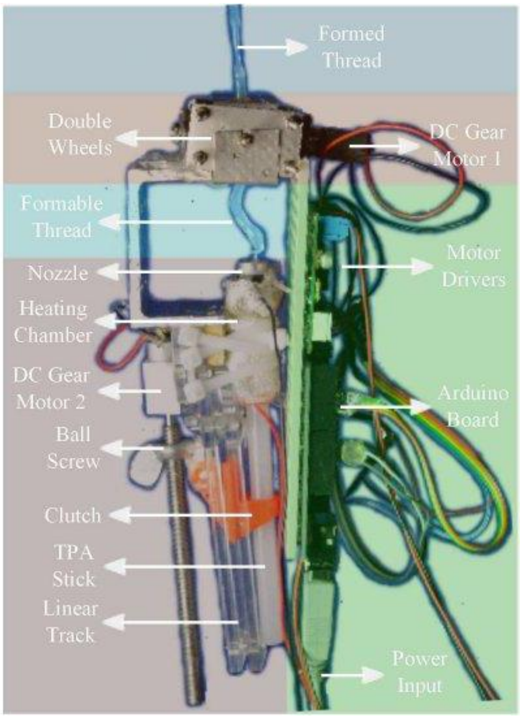

Fig. 3. A thread-forming robot (front view).

TABLE II
ROBOT SPECIFICATION

Mass	300 g
Dimension (width, thickness, height)	6×4×18 cm^3
Inner diameter of nozzle exit D_{ni}	4 mm
TPA supply and deformation temperature T_{sup}	60-70°C
Number of DC gearmotors	2
Thread diameter D_{ft} range	1.1-4.5 mm
Power consumption	2.5 W
Average descending speed	0.73 cm/min

where c is specific heat capacity of the material, h is convective heat transfer coefficient, K is thermal conductivity of the material, and A_{conv} is surface area of heat being convected and A_{cond} is surface area of heat being conducted. In the case of a cylindrical thread, A_{conv} corresponds to the outer surface of the cylinder while A_{cond} corresponds to the cross section:

$$A_{conv} = \pi D_{ft} L, A_{cond} = \frac{\pi D_{ft}^2}{4}$$

Assuming source material is supplied and immediately deformed and Δt_I, Δt_{II} are both very short, (2) can be solved with initial condition of $T(0) = T_{sup}$:

$$T(t) = C_0 - C_1 \cdot e^{-C_2 t} \tag{3}$$

where

$$C_0 = \frac{KT_{sup}D_{ft} + 2L^2 T_{amb} h}{2hL^2 + KD_{ft}}$$

$$C_1 = \frac{2L^2 h(T_{amb} - T_{sup})}{2hL^2 + KD_{ft}}, C_2 = \frac{2(2hL^2 + KD_{ft})}{L^2 c D_{ft} \rho}$$

III. ROBOT DESIGN AND CONTROL

A robot is designed and prototyped to demonstrate the feasibility of the technology (Fig. 3). The robot weighs ca. 300 gram and has an overall dimension of 6×4×18 cm^3 (width, thickness, height). The robot consists of three main parts i.e. a material supply mechanism, a coupled deformation-locomotion mechanism, and an electronics unit. The material supply mechanism contains TPA material (GG02, Dremel, USA) in a cylindrical shape (ø7 mm). The deformation-locomotion mechanism has one degree of freedom to enable the robot to elongate supplied material as well as moving along a formed thread. The three parts are arranged in such a way that the deformation-locomotion mechanism is on the top, and the material supply mechanism and the electronics unit are on the two sides below with the TPA stick in the central vertical axis. The material supply mechanism and the deformation-locomotion mechanism are connected by a rigid aluminium piece so that the exit of the nozzle is placed 3 cm under the bottom of the deformation-locomotion mechanism. This distance determines the maximal length of the thread before it gets grabbed by the robot. All three parts are described in detail in this section.

A. Material Supply Mechanism

The material supply mechanism can be described as a solid TPA stick delivered linearly through a heating chamber and then pushed out of a nozzle (Fig. 3). Linear delivery is converted from a DC gear motor's rotation through a ball screw fixed with a TPA stick clutch. The clutch is constrained with only linear motion by a linear track, at the end of which the DC gear motor (DC gear motor 2) is anchored. The heating chamber is an aluminium cavity with an opening of 9 mm in diameter at one end and a nozzle with D_{ni}=4 mm at the other end. The cavity is heated by six 10-Ω power resistors connected in parallel and placed tightly around its outer surface and covered by an insulating glass fibre cloth. The TPA stick is held by the clutch at one end and inserted into the aluminium cavity at the other end through a silicone tube for leakage prevention. The design is similar to the one presented in [12] but smaller. The TPA stick clutch and the silicone tube are adopted from a commercial hand-held glue gun, while the linear track is laser cut out from a 4-mm thick plate of Polymethyl-methacrylate (PMMA). The whole mechanism is manually assembled mostly with screws, except that the heating chamber is fixed at one end of the linear track with plastic binders.

B. Deformation-Locomotion Mechanism

The deformation-locomotion mechanism consists of a two cylindrical wheel track system which is run by DC gear motor 1 (250:1 Micro Metal Gearmotor HP, Pololu, USA), whose details can be seen in Fig. 4. One of the wheels (right) is fixed on the motor's shaft, which is fixed on the surrounding walls of the covering metal box. The other wheel (left) is attached on a shaft which can move linearly on a track with a fixed length L_{tr} on the surrounding walls. The end points of the left wheel's shaft are attached onto the box

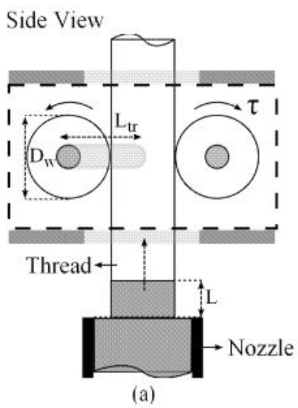

Fig. 4. Side view (a) and top/bottom view (b) of the deformation-locomotion mechanism

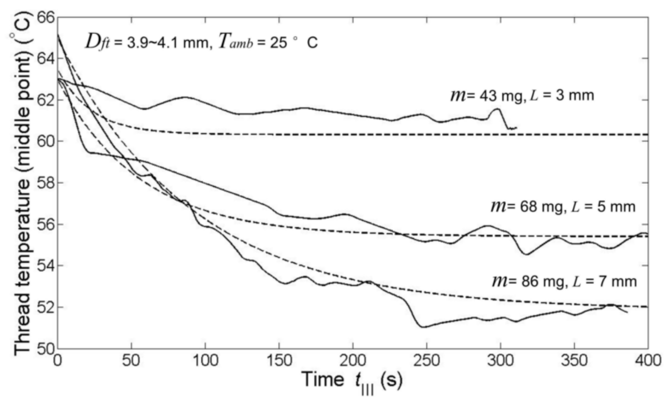

Fig. 5. Results of thermodynamics in phase transition of formed threads.

with springs, which pull the wheel towards the center of the mechanism. The track constraints this wheel to move along a linear route while springs allow it to passively adjust to the changing diameter of the formed thread. The spring force F, shown in Fig. 4b is in linear relation with gap between the two wheels or in other words with the diameter of the formed thread D_{ft}. This force constitutes the normal force which generates the friction between the formed thread and the wheels, which helps the overall mechanism to hold onto the formed thread while compensating for the weight of the robot and potential payload. Springs are chosen so that this friction force is greater than the weight of the mechanism while the wheels are turning or not.

Since the mechanism realizes deformation at the same time of locomotion, by assuming no slip between the wheels and a thread, the deformed length L of a new thread can be expressed by the rotational distance of the wheels;

$$L = \pi D_w f \Delta t_{II} \tag{4}$$

where f is revolutions per unit time for DC gearmotor 1, which is 120 r/min at 6 V. Fig. 4a shows that gearmotor 1 rotates the right wheel in the clockwise direction to deform the thread as well as to move the robot downwards on the formed thread.

The deformation-locomotion mechanism is completed with two constraining plates on top and bottom of the structure with a hole of diameter $D_{ch} = 1.2cm$ to keep the formed thread within the central axis which goes through the center of mass of the whole system. Although this limits the maximum possible thread diameter, it helps the robot to be in balance during locomotion.

C. Electronics and Control

An microcontroller board (Arduino Duemilanove, Italy) is used to control both gearmotors which are each driven by a standard motor driver (iMDs03, iXs Research Inc., Japan) with PWM signals. The microcontroller board is powered by a USB cable to a laptop, while the two motor drivers are connected to an external power supply. The heaters are connected to a second external power supply, and it was found that a power of 2.3-2.5 W can self-stabilize T_{sup} at 60-70 °C which was found to be an adequate for material supply and deformation.

A control programme is preloaded onto the microcontroller board. The programme implements a simple open-loop controller: After preparation of preheating the chamber to T_{sup}, the robot starts to supply TPA by switching on DC gearmotor 2 for Δt_I. It then rotates the wheels by switching on DC gearmotor 1 for Δt_{II} for deformation and locomotion. The controller continues with a waiting time period of Δt_{III} for cooling down the formed thread, and then starts the next repetition.

IV. EXPERIMENTS AND RESULTS

To assess the thread formation and locomotion performance of the robot, experiments have been conducted to measure the phase transition time as well as variability and repeatability of thread diameter. In all experiments, the robot starts with holding onto an existing thread of TPA hanging from the ceiling at room temperature (T_{amb}=25 °C). In this section, experimental methods and results are presented.

A. Phase Transition Time

Phase transition time is important for determining control parameter Δt_{III} in thread formation. Therefore experiment was firstly conducted to validate the thermodynamics model of phase transition through cooling in Section II.B. Specifically, we look into how the amount of TPA affects the cooling time. In the experiment, T_{sup} was set to be 63-65°C, TPA of three different mass was supplied with Δt_I of 0.9, 1.5, and 2.0 seconds, and then immediately deformed with different L into a given diameter of 4 mm. The temperature change of the formed thread was measured by an external thermal imager (TIM 160, Micro-Epsilon, Germany). The measuring point was set at the middle section of the thread, which corresponds to 1.5, 2.5, and 3.5 mm above the nozzle exit for the three cases.

Fig. 5 shows the experimental result. In each case, a TPA mass of 43, 68, and 86 mg was supplied and deformed into a diameter of 3.9-4.1 mm. The dashed lines show theoretical approximation based on (3), and the curve fitting parameters

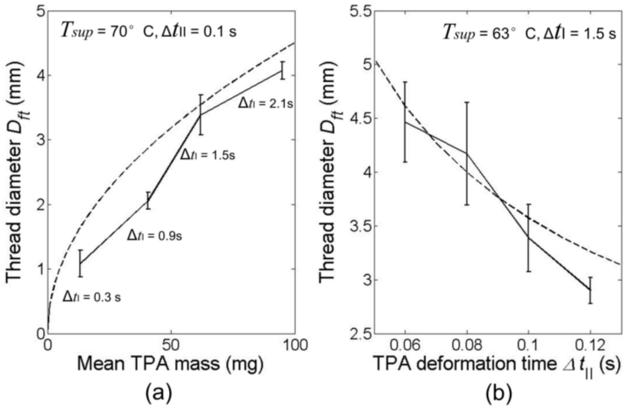

Fig. 6. Results of diameter variation in formed threads by the robot.

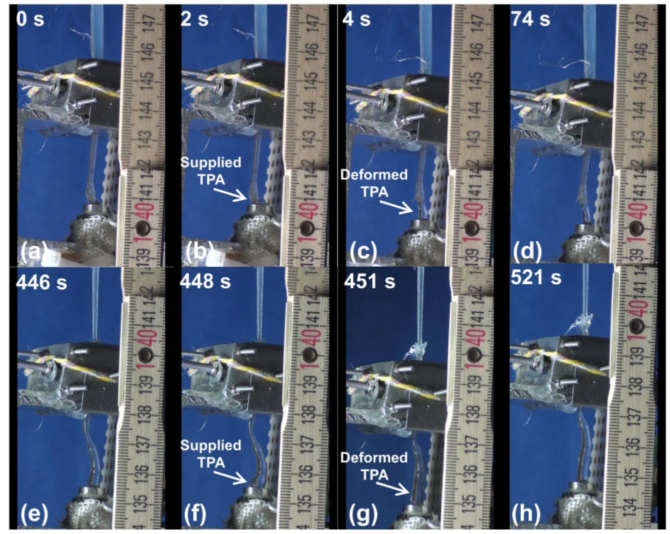

Fig. 7. Snapshots of two repetitions of thread formation and descending in Trial 7. (a)-(d) shows the first repetition of thread formation and locomotion, with (a)-(b), (b)-(c), (c)-(d) showing subprocess I, II, III respectively. (e)-(h) shows the seventh repetition of the trial, where the formed thread could be seen to pass the deformation-locomotion mechanism, suggesting that the robot had successfully held and moved on the formed thread.

are indicated in Table I. It took approximately 180 seconds for the temperature of threads to reach a steady state. This steady state was not room temperature because of continuous energy input from the nozzle. Given the same diameter, the temperature in the steady state is lower for larger amount of TPA due to the resulting larger surface area of thermal convection A_{conv}. Further cooling will require repetition of TPA supply and deformation, so that a previously formed section can be moved further away from the nozzle. This result indicates that as long as the diameter of the thread is the same, the more TPA supplied and deformed at a given temperature, the faster it cools. The values helped determining control parameters in the experiment of repeated thread formation and locomotion in Section IV.C.

B. Variability of Thread Diameter

As introduced in Section I, the proposed technology aims at varying thread diameter for wider coverage of potential payload. Two sets of experiments were therefore carried out to measure the variability in diameter of formed thread. In both sets of experiments, the temperature of TPA supply T_{sup} was set to be between 60-70°C. In the first set of experiment the amount of supplied TPA was varied while elongation was kept the same. In order to achieve that, DC gearmotor 2 was controlled to push TPA stick for different time periods Δt_I between 0.3 and 2.1 seconds, and elongation was enabled by turning on DC gearmotor 1 for Δt_{II}=0.1 s. In the second set of experiment, the supply Δt_I was kept 1.5 seconds, while elongation was varied by setting Δt_{II} between 0.06 and 0.12 seconds. For each Δt_I or Δt_{II}, three trials were made, and after each trial the formed threads were removed and their mass and diameter were measured with a high-precision scale (Voltcraft PS-20) and a digital Vernier scale.

Fig. 6a shows the diameter variation from the first set of experiment. For Δt_I of 0.3, 0.9, 1.5, and 2.1 seconds, the mass m of supplied TPA was 13.3±1.5, 40.7±3.8, 62.0±5.0, and 95.0±5.0 mg. Diameter of formed threads was 1.1±0.2, 2.1±0.1, 3.4±0.3, and 4.1±0.1 mm respectively. In the figure, theoretical estimation from geometrical relationship (1) are also plotted with m from 0 to 100 mg and L calculated from (4). It can be seen that experimental data fits (1) well.

Fig. 6b shows the diameter variation from the second set of experiment. For Δt_{II} of 0.06, 0.08, 0.10, and 0.12 seconds, the diameter of formed threads was 4.5±0.4, 4.2±0.5, 3.4±0.3, and 2.9±0.1 mm respectively. In the figure, theoretical estimation from geometrical relationship (1) are also plotted with m=63 mg (experimental data 63.2±5.0 mg) and L calculated from (4) with Δt_{II} from 0.05 to 0.13 seconds. It can be seen that experimental data also follows geometrical estimation.

Comparing the results from the two sets of experiment: Values for experimental data are slightly lower than geometrical estimation, which may be explained by slight inconsistency in diameter between the end and the middle section of the thread. Varying the mass of supplied TPA has lower standard deviations than varying the deformation length, which could be caused by slip between the thread and the two wheels and violation of (4). In all, a diameter range of 1.1-4.5 mm have been achieved for formed threads. This result implies an estimated range of 0.5-8 kg for a combination of payload and robot body mass, when TPA tensile strength is taken as 5 MPa at room temperature.

C. Repeatability of Thread Formation

Seven trials of repeated thread formation were carried out to assess the repeatability. In all trials, T_{sup} was set to be 65°C, and Δt_{III} in each repetition was set to be 60-70 seconds. Δt_I was varied between 1.3 and 2 seconds and Δt_{II} was varied between 0.15 and 0.25 seconds.

All trials succeeded with 3-11 repetitions, which results in a record of a 10-cm thread automatically formed by the robot while locomotion. Fig. 7 shows resulting snapshots of

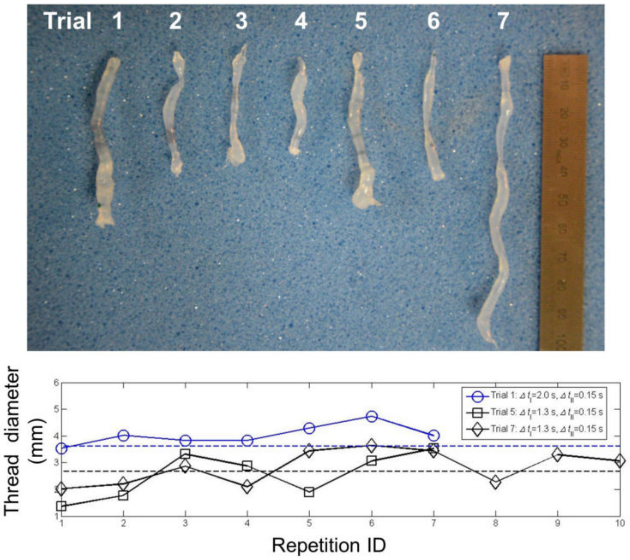

Fig. 8. Experiment results of repeatability of thread formation.

one of the trials (Trial 7) where Δt_I and Δt_{II} were set to 1.3 s and 0.15 s respectively. Fig. 7a-d shows the first repetition of thread formation and locomotion, with a-b, b-c, c-d showing subprocess I, II, III respectively. Fig. 7e-h shows the seventh repetition of the trial, where the formed thread passed the deformation-locomotion mechanism, suggesting that the robot had successfully held and moved on the thread formed by itself (also see a supplementary video showing from the second to the eighth repetition from the same trial). From this figure, we can also see that in each repetition the robot descended 0.9 cm, which means an average locomotion speed of 0.73 cm/min has been achieved including thread formation.

Fig. 8 shows resulting threads from the seven trials, as well as quantitative data of repeatability from three of the trials (Trial 1, 5, 7) where thread diameters were measured for each repetition. For the three measured trials, the diameters were 4.0±0.4 mm, 3.3±0.8 mm and 2.9±0.6 mm respectively. The estimated value for each trial is indicated by a dashed line, which is closely placed to experimental data. The result suggests a relative deviation of 10-25% between repetitions. The deviation came from TPA supply and deformation length as shown in Section IV.B, and physical interactions between the formed thread and the deformation-locomotion mechanism. The values may be used to set safety margins for a target diameter given a target payload.

V. CONCLUSIONS AND FUTURE WORK

The paper proposed a new concept of locomotion in a free-space for mobile robots. The concept is inspired by spiders' behaviour of forming silks into threads to move around in a 3D space. Compared to using an existing onboard cable with a fixed diameter, the proposed approach enables variation of thread diameter through formation from onboard source material. Thus it provides wider coverage of payload by mobile robots. As a first step, a case of descending locomotion with inverted thread formation has been studied. Technology has been developed for inverted thread formation with TPA material through thermally induced phase transition. To demonstrate the feasibility of the technology, a 300-gram robot has been designed and prototyped. Experiments have been carried out with the robot in room-temperature environment to assess the performance of thread formation and locomotion. Results suggest repeatable inverted thread formation with a diameter range of 1.1-4.5 mm. With a power consumption of 2.5 W, a locomotion speed of 0.73 cm/minute has been achieved.

Given the results, many directions of future work can be foreseen. For example, locomotion speed and consistency in formed threads may be improved with sensory feedback control based on solid material models [13]; the double-wheel mechanism can be replaced by legs, so that the robot can cross over two threads and enables formation of a small-scale cross network; microrobot technologies [14] may be used to make the robot lighter and smaller, etc. An improved robot prototype may be also used as a controlled physical model to investigate biological questions with spiders.

REFERENCES

[1] S. Hirose, A. Nagakubo, and R. Toyama, "Machine that can walk and climb on floors, walls and ceilings," in Proc. 5th Int. Conf. Advanced Robotics, Pisa, 1991, pp. 753-758.

[2] R. Molfino, M. Armada, F. Cepolina, M. Zoppi, "Roboclimber the 3 ton spider," Ind. Robot, Vol. 32, No. 2, pp. 163-170, 2005.

[3] M. Bonani, S. Magnenat, P. Retornaz, and F. Mondada, "The Hand-Bot, a robot design for simultaneous climbing and manipulation," in Proc. 2nd Int. Conf. Intelligent Robotics and Applications, Singapore, 2009, pp. 11-22.

[4] A. L. Desbiens, A. T. Asbeck, and M. R. Cutkosky, "Landing, perching and taking off from vertical surfaces," Int. J. Robot. Res., vol. 30, no. 3, pp. 355-370, Mar. 2011.

[5] M. Xu and R. V. Lewis, "Structure of a protein superfiber: Spider dragline silk," Proc. Natl. Acad. Sci. U.S.A., vol. 87, no. 18, pp. 7120-7124, Sep. 1990.

[6] F. Vollrath, "Biology of spider silk," Int. J. Biol. Macromol., vol. 24, no. 2-3, pp. 81-88, Mar. 1999.

[7] L. Wang and F. Iida, "Physical connection and disconnection control based on hot melt adhesives," IEEE-ASME Trans. Mechatron., vol. 18, no. 4, pp. 1397-1409, Jun. 2012.

[8] L. Wang, L. Graber and F. Iida, "Large-payload climbing in complex vertical environments using thermoplastic adhesive bonds," IEEE Trans. Robot., vol. 29, no. 4, Apr. 2013.

[9] C.A. Mahieux, "A systematic stiffness-temperature model for polymers and applications to the prediction of composite behavior," Ph.D. dissertation, Dept. Materials Eng. Sci., Virginia Tech, Cambridge, VA, 1999.

[10] M.L. Williams, R.F. Landel, and J.D. Ferry, "The temperature dependence of relaxation mechanisms in amorphous polymers and other glass-forming liquids," J. Am. Chem. Soc., vol. 77, no. 14, pp. 3701-3707, Jul. 1955.

[11] S. Yamakawa, "Hot-melt adhesive bonding of polyethylene with ethylene copolymers," Polym. Eng. Sci., vol. 16, no. 6, Jun. 1976.

[12] M. Osswald and F. Iida, "A climbing robot based on hot melt adhesion," in Proc. 2011 IEEE/RSJ Int. Conf. Intelligent Robots and Systems, San Francisco, pp. 5107-5112.

[13] A. Khan and H. Zhang, "Finite deformation of a polymer: Experiments and modeling," Int. J. Plasticity, vol. 17, no. 9, pp. 1167-1188, Sep. 2001.

[14] R. Sahai, S. Avadhanula, R. Groff, E. Steltz, R. Wood, and R. S. Fearing, "Towards a 3g crawling robot through the integration of microrobot technologies," Proc. 2006 IEEE Int. Conf. Robotics and Automation, Orlando, pp. 296-302.